Structural Characteristics of Size-Controlled Self-Aggregates of Deoxycholic Acid-Modified Chitosan and Their Application as a DNA Delivery Carrier

ARTICLE *in* BIOCONJUGATE CHEMISTRY · NOVEMBER 2001

Impact Factor: 4.51 · DOI: 10.1021/bc015510c · Source: PubMed

8 AUTHORS, INCLUDING:

Se Hoon Gihm
Seoul National University
8 PUBLICATIONS **359** CITATIONS
SEE PROFILE

Chong Rae Park
Seoul National University
160 PUBLICATIONS **2,970** CITATIONS
SEE PROFILE

Kye Young Lee
Konkuk University Medical Center
81 PUBLICATIONS **2,050** CITATIONS
SEE PROFILE

Ick Chan Kwon
Korea Institute of Science and Technology
360 PUBLICATIONS **14,825** CITATIONS
SEE PROFILE

Structural Characteristics of Size-Controlled Self-Aggregates of Deoxycholic Acid-Modified Chitosan and Their Application as a DNA Delivery Carrier

Young Hyo Kim, Se Hoon Gihm, and Chong Rae Park*

Enviro-Polymers Design Laboratory, Hyperstructured Organic Materials Research Center (HOMRC) and School of Materials Science and Engineering, Seoul National University, Seoul 151-744, Korea

Kuen Yong Lee,† Tae Woo Kim, Ick Chan Kwon, Hesson Chung, and Seo Young Jeong

Biomedical Research Center, Korea Institute of Science and Technology, P.O. Box 131, Cheongryang, Seoul 130-650, Korea. Received April 30, 2001; Revised Manuscript Received August 16, 2001

Precise control of the size and structure is one critical design parameter of micellar systems for drug delivery applications. To control the size of self-aggregates, chitosan was depolymerized with various amounts of sodium nitrite, and hydrophobically modified with deoxycholic acid to form self-aggregates in aqueous media. Formation and physicochemical characteristics of size-controlled self-aggregates were investigated using dynamic light scattering, fluorescence spectroscopy, and computer simulation method. The size of self-aggregates varied in the range of 130−300 nm in diameter, and their structures were found to depend strongly on the molecular weight of chitosan ranging from 5 to 200 kDa. Due to the chain rigidity of chitosan molecule, the structure of self-aggregates was suggested to be a cylindrical bamboolike structure when the molecular weight of chitosan was larger than 40 kDa, which might form a very poor spherical form of a birdnestlike structure. To explore the potential applications of self-aggregates as a gene delivery carrier, complexes between chitosan self-aggregates and plasmid DNA were prepared and confirmed by measuring the fluorescence intensity of ethidium bromide and electrophoresis on agarose gels. The complex formation had strong dependency on the size and structure of chitosan self-aggregates and significantly influenced the transfection efficiency of COS-1 cells (up to a factor of 10). This approach to control the size and structure of chitosan-derived self-aggregates may find a wide range of applications in gene delivery as well as general drug delivery applications.

INTRODUCTION

Colloidal systems have found numerous applications as promising delivery vehicles of drugs, proteins, antigens, and genes due to their reduced toxic side effect and improvement of therapeutic effect (*1*, *2*). Polymeric self-assembly systems, as one of colloidal systems, have been widely investigated in terms of their micellar behavior as well as their application to the fields of biotechnology and pharmaceutics (*3*−*5*). Polymeric self-assemblies are usually formed from block copolymers (*6*−*8*) or hydrophobically modified water-soluble polymers (*9*−*11*). It may be fascinating to develop polymeric self-aggregates from hydrophobically modified water-soluble polymers rather than block copolymers, as it is generally difficult to synthesize new types of block copolymers.

One attractive utilization of polymeric self-aggregates to date is as a gene delivery vehicle in order to cure many hereditary diseases and treat acquired disease resulting from either multigenetic disorders or foreign viral genes (*12*, *13*). Viral delivery systems have many advantages for gene delivery due to their high efficiency and wide range of cell targets. However, they have some drawbacks of immune responses and oncogenic effect in vivo. Nonviral delivery systems including cationic liposomes and polymeric systems have therefore been extensively investigated (*14*−*18*). Cationic liposomes are widely applicable to many animal cells due to their nonspecific ionic interaction and low toxicity. However, due to the poor stability in vivo of cationic liposomes, many polymeric systems have been studied as alternatives for in vivo and in vitro applications (*16*−*18*).

Chitosan is generally considered biocompatible, biodegradable, and of low toxicity (*19*). In addition, chitosan has cationic characters even in neutral condition to form complexes with negatively charged plasmid DNA, and promotes cell transfection (*20*−*23*). We have previously demonstrated that self-aggregated nanoparticles, prepared from hydrophobically modified chitosan, could find a potential application as a gene delivery vehicle, due to the controlled complex formation with plasmid DNA (*24*). However, the size of the chitosan self-aggregates was not precisely controlled by varying the degree of substitution, pH, and/or ionic strength of the medium, probably due to the rigidity of chitosan backbone chain, and their diameter was in the range of 160−180 nm (*10*, *24*). To be used as a delivery vehicle, the size of self-aggregates should be more precisely controlled, and their structure should be further investigated.

* To whom correspondence should be addressed. Phone: +82 2 880 8030. Fax: +82 2 885 1748. E-mail: crpark@gong.snu.ac.kr.

† Present address: Departments of Biologic & Materials Sciences and Chemical Engineering, University of Michigan, Ann Arbor, MI 48109.

[1] Abbreviations used: DAMC, deoxycholic acid-modified chitosan; DPH, 1,6-diphenyl-1,3,5-hexatriene; DS, degree of substitution; EDC, 1-ethyl-3-(3-dimethylaminopropyl)carbodiimide; EtBr, ethidium bromide; PEO, poly(ethylene glycol).

10.1021/bc015510c CCC: $20.00
Published on Web 11/03/2001

It is thus the aim of this paper to control the size and its distribution of self-aggregates of deoxycholic acid-modified chitosan (DAMC) and to verify their structure in order to utilize as a gene delivery carrier. In brief, chitosan was depolymerized using sodium nitrite and modified with deoxycholic acid in the presence of carbodiimide. We hypothesized that the chitosan derivatives could form self-aggregates with different sizes and structures, depending on the molecular weight of chitosan. Micellar characteristics were investigated by fluorescence spectroscopy, dynamic light scattering method, and computer simulation. In addition, the chitosan self-aggregates were considered to form complexes with plasmid DNA by ionic interactions. Complexation behavior between plasmid DNA and chitosan self-aggregates, as well as their transfection activity, were investigated and interpreted in relation to their micellar structures.

MATERIALS AND METHODS

Materials. Chitosan (M_w = 1.0 × 10^6, degree of deacetylation = 80%) was purchased from Fluka (Milwaukee, WI). Sodium nitrite, deoxycholic acid, ethidium bromide, and 1-ethyl-3-(3-dimethylaminopropyl)carbodiimide (EDC) were purchased from Sigma (St. Louis, MO) and used without further purification. Pyrene and 1,6-diphenyl-1,3,5-hexatriene (DPH) were purchased from Aldrich (St. Louis, MO) and used as a fluorescence probe. DNA molecular weight marker II (λDNA/Hind III digested) was purchased from Boehringer Mannheim GmbH (Germany). The water was purified by distillation, deionization, and reverse osmosis (MilliQ Plus).

Depolymerization of Chitosan. Chitosan was dissolved in a 2% acetic acid solution and treated for 3 h at room temperature with different amounts of sodium nitrite in a range from 0.01 to 0.25 mol/mol glucosamine residues. The resulting solution was neutralized with a 1.0 N sodium hydroxide solution, precipitated with acetone, and dried in a vacuum at room temperature. The molecular weight of the depolymerized chitosan was determined by gel permeation chromatography (GPC) through Ultrahydrogel linear columns (Waters, USA) at a flow rate of 1.0 mL/min. A buffer solution of 0.15 M acetic acid and 0.5 M sodium acetate was used as a mobile phase. Pullulan (Showa, Japan) was used as a molecular weight standard. Degree of deacetylation of chitosan was determined by the titration method as previously reported (*25*).

Synthesis of Deoxycholic Acid-Modified Chitosan (DAMC). The depolymerized chitosan was hydrophobically modified with deoxycholic acid (0.05−0.34 mol/mol glucosamine residues of chitosan) in the presence of EDC for 24 h at room temperature (*24*). The reaction mixture was poured into a methanol/ammonia solution (7/3, v/v). The precipitates were filtered off, washed thoroughly with methanol and ether, and then followed by vacuum-drying at room temperature. The degree of substitution, defined as the number of deoxycholic acid groups per 100 anhydroglucose units of chitosan, was determined by calculation of the C/N ratio from an elemental analyzer (LECO). Infrared spectra of chitosan derivatives were monitored on an FT-IR spectrophotometer (resolution, 4 cm^{-1}; 32 scans; MIDAC) to confirm the conjugation reaction between chitosan and deoxycholic acid (KBr pellet: 1655 (NHC═O) cm^{-1}).

Preparation of DAMC Self-Aggregates. DAMC was suspended in a phosphate-buffered saline (PBS) solution (pH 7.2) under gentle shaking at 37 °C for 48 h, followed by sonication using a probe type sonifier (Sigma Ultrasonic Processor, GEX-600) at 30 W for 2 min. The sonication was repeated three times to get an optically clear solution. To inhibit the heat build-up during sonication, the pulse function was used (pulse on, 5.0 s; pulse off, 1.0 s) (*10*).

Fluorescence Measurements. Fluorescence spectra of DAMC self-aggregate solutions, which contained 6.0 × 10^{-7} M of pyrene as a probe, were obtained with an ISS K2 fluorometer (ISS, Champaign, IL). For the measurement of the intensity ratio of the first and the third highest energy bands in the pyrene emission spectra, the slit openings were set at 1 mm (excitation) and 0.5 mm (emission). The excitation wavelength (λ_{ex}) was 336 nm, and the spectra were accumulated with an integration time of 5 s/nm.

Assuming simple partition equilibrium, the equilibrium constant (K_v) for partitioning of pyrene between water and micellar phases was calculated according to the method of Wilhelm et al. (*26*)

$$\frac{F - F_{min}}{F_{max} - F} = \frac{K_v x c}{1000\rho} \quad (1)$$

where F is the intensity ratio (= I_{336}/I_{333}) from the fluorescence excitation spectrum at the intermediate concentration range of DAMC (λ_{em} = 390 nm), F_{min} and F_{max} are the intensity ratios at low concentration and at high concentration, respectively, x is the weight fraction of deoxycholic acid in DAMC, and ρ is the density of the inner core of self-aggregates that is assumed to be the same value of deoxycholic acid in water (= 1.31 g/mL) (*27*).

Fluorescence anisotropy of the DAMC self-aggregate solution containing DPH (2.1 × 10^{-6} M) was measured using L-format geometry of detection (λ_{ex} = 360 nm, λ_{em} = 430 nm). Fluorescence anisotropy (r) was calculated from the following relationship.

$$r = \frac{(I_{VV} - I_{VV}^{s}) - G(I_{VH} - I_{VH}^{s})}{(I_{VV} - I_{VV}^{s}) + 2G(I_{VH} - I_{VH}^{s})} \quad (2)$$

where I^s is the contribution of scattered light from a sample solution in the absence of DPH, G (= I_{VH}/I_{HH}) is an instrumental correction factor, and I_{VV}, I_{VH}, I_{HV}, and I_{HH} correspond to the resultant emission intensity polarized in the vertical or the horizontal detection planes (the second subscript) when excited with vertically or horizontally polarized light (the first subscript) (*28*).

Dynamic Light-Scattering Measurement. An argon ion laser (Lexel Laser Model 95) was operated at a wavelength of 488 nm. The intensity autocorrelation was measured with a Brookhaven BI-9000AT digital autocorrelator (θ = 90°, T = 25 ± 0.1 °C). A nonlinear regularized inverse Laplace transformation technique (CONTIN) was used to obtain the distribution of decay function. Mean diameter (d) was calculated from the Stokes−Einstein equation.

Computer Simulation. Based on the experimentally observed data, the structures of native chitosan, DAMC, and DAMC self-aggregate were simulated using Cerius2 programs that contain the modules such as polymer builder, open force field, energy minimizer, and molecular dynamics (MSI, San Diego, CA). Chitosan and DAMC were initially created on a computer and energy-minimized using the modules of polymer builder and energy minimizer. The micellar structure of DAMC was obtained from the molecular dynamics simulation method

for 20 ps (20000 steps × 0.001 ps/step) using Dreiding 2.21 force field and Universal 1.02 force field.

Plasmid DNA. The pCMV−Luc+, obtained from the plasmid pGL3 (Promega, Madison, WI) using Xba I and Hind III, consists of a cytosolic form of *Phontinus pyralis* luciferase cDNA (*29*). The plasmid was amplified in the *Escherichia coli* DH5-α strain and purified by a Qiagen kit (Chatsworth, CA) according to the manufacturer's instruction. DNA purity was determined by measuring the optical density (OD), and DNA with $OD_{260}/OD_{280} \geq 1.8$ was used.

Characterization of DAMC Self-Aggregate/DNA Complexes. Complexes were prepared by the addition of DNA solution (0.1 μg/mL) to DAMC self-aggregate solution (1 mg/mL) at different charge ratios, following incubation for 20 min at room temperature. The charge ratio (±) was defined as the ratio of the number of amino groups in DAMC self-aggregates to the number of phosphate groups in DNA. Both DNA and DAMC self-aggregate solutions were prepared in PBS solution, and the final volume of the complexes was 25 μm. Complex formation between plasmid DNA and DAMC self-aggregates was confirmed by electrophoresis using agarose gels as previously reported (*24*). The DAMC self-aggregate/DNA complexes were further characterized by fluorescence spectroscopy. Briefly, the complex solution containing EtBr (2 nmol) was incubated for 10 min, and the fluorescence intensity was measured using the ISS K2 fluorometer at $\lambda_{ex} = 488$ nm (slit width 2.0 mm) and $\lambda_{em} = 594$ nm (slit width 1.0 mm) ($n = 3$).

Cell Culture and In Vitro Transfection. A simian kidney cell line (COS-1) was cultured in the Dulbecco's modified Eagle's medium (DMEM) supplemented with 10% fetal bovine serum (FBS) at 37 °C in a humidified 5% carbon dioxide incubator. Cells were seeded at 2×10^4 cells per well of a 96-well plate 12 h before transfection. Cells were 70−80% confluent at the time of transfection. The plasmid of pCMV−Luc+ (0.5 μg) was mixed with the DAMC self-aggregate solution at a charge ratio of 4 in the absence of serum and added to the single well. Naked DNA was also used as a control. After 1 h incubation, the cells were washed with serum-free DMEM to remove the remaining complexes, fed again with fresh media containing FBS, and cultured for 24 h after transfection. The transfected cells were assayed for luciferase activity using a Promega kit (Madison, WI) with a luminometer (Turner Designs Luminometer Model TD-20/20, Promega). The luciferase content was calculated from the relative light units using a standard curve obtained from the purified firefly luciferase (Sigma). The background level of luciferase activity in untreated cell lysates was measured from the organs of mice without any treatment and found to be negligible.

RESULTS AND DISCUSSION

Depolymerization and Hydrophobic Modification of Chitosan. Chitosan was depolymerized using sodium nitrite to obtain samples with various molecular weights. The depolymerization reaction was selective and could be easily controlled by adjusting the amount of sodium nitrite used in the reaction. The weight average molecular weights of the depolymerized chitosans, determined by GPC, were in the range of 5−200 kDa and the polydispersity of about 2. However, their degree of deacetylation was not significantly affected by the depolymerization reaction in this range of molecular weights (Figure 1).

The depolymerized chitosan was hydrophobically modified with deoxycholic acid in the presence of EDC, which

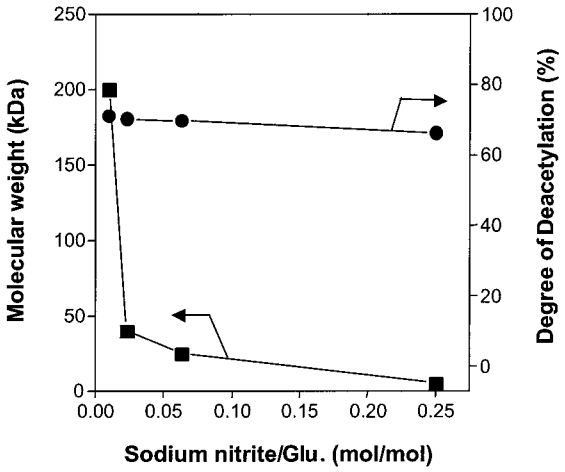

Figure 1. Changes of the molecular weight and the degree of deacetylation of depolymerized chitosans.

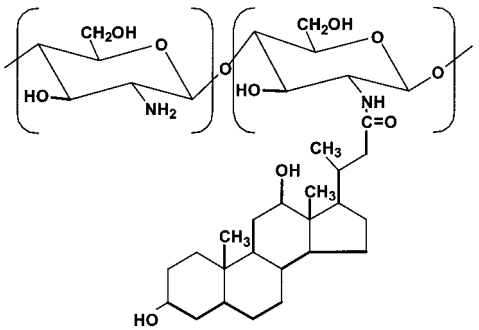

Figure 2. Chemical structure of deoxycholic acid-modified chitosan (DAMC).

Table 1. Characteristics of Chitosan Self-aggregates with Different Molecular Weights

sample[a]	$cac^b \times 10^2$, mg/mL	$K_v^c \times 10^{-5}$	r[d]	d^e, nm	d_{real}/d_{cal}[f]
DAMC5k	6.7	0.8	0.186	132	40
DAMC25k	4.0	1.2	0.246	170	10
DAMC40k	2.3	2.5	0.302	230	9
DAMC200k	1.2	3.9	0.340	300	2

[a] Deoxycholic acid-modified chitosan (DAMC) with DS = 6.0. [b] Critical aggregation concentration. [c] Equilibrium binding constant of pyrene according to eq 1. [d] Anisotropy value of DPH according to eq 2. [e] Mean diameter measured by dynamic light-scattering method. [f] Minimum aggregation number of chitosan molecular chains calculated on the assumption of the formation of a spherical unimer micelle.

is known to promote amide linkage formation between amine and carboxylic acid (*30*). EDC initially reacts with the carboxyl group of deoxycholic acid to form an active ester intermediate, and the intermediate readily reacts with a primary amine of chitosan as a result of amide linkage formation (Figure 2). The characteristic peak at 1655 cm^{-1} from FT-IR spectra confirmed the amide bond formation between chitosan and deoxycholic acid (data not shown). The degree of substitution (DS) increased with increasing mole ratio of deoxycholic acid and was in the range from 2 to 10. The chitosan derivatives with DS = 6 of various molecular weights were used in this study in order to investigate the effect of the molecular size on self-aggregate formation in aqueous media. The number following the sample code DAMC in Table 1 indicates the molecular weight of chitosan.

Characteristics of DAMC Self-Aggregates. The self-aggregation behavior of DAMC in aqueous media was initially investigated by a fluorometry in the presence of

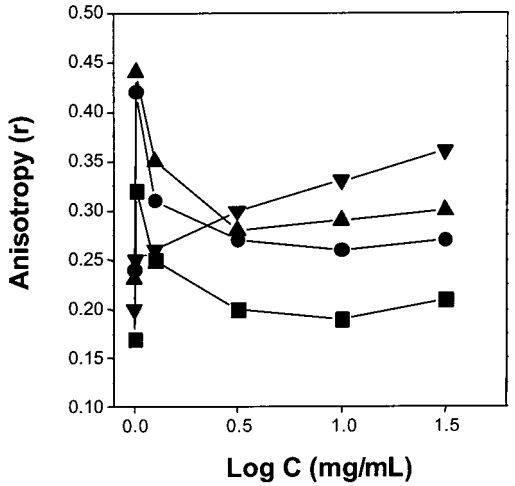

Figure 3. Changes of the anisotropy value (*r*) for DPH in the presence of DAMC self-aggregates in PBS solution (■, DAMC5k; ●, DAMC25k; ▲, DAMC40k, ▼, DAMC200k).

pyrene as a fluorescent probe. Pyrene is poorly soluble in water, but strongly emits when the self-aggregates or other hydrophobic microdomains are formed in an aqueous solution, as it preferably lies close to (or inside) the microdomains (*28*). The intensity of the third highest vibrational band as well as the total emission intensity of pyrene started to drastically increase over a certain concentration of DAMC, which was defined as a critical aggregation concentration (*cac*). The *cac* was determined from the intensity ratio (I_1/I_3) of the first (372 nm) and the third (383 nm) highest energy band in the emission spectra of pyrene. The *cac* values of DAMC self-aggregates were in the range of $1.2-6.7 \times 10^{-2}$ mg/mL, depending on the molecular weight of chitosan (Table 1). Since the unmodified chitosan did not form self-aggregates, it was used as a control.

Polarity of the inner core of self-organized structure is one important factor in its application as a drug delivery vehicle. Polarity of DAMC self-aggregates can be expressed with an equilibrium constant (K_v) of pyrene. In principle, the higher K_v value implies the lower polarity. So, the K_v value increasing with the molecular weight of chitosan indicates the existence of less polar microdomains inside the self-aggregates (Table 1).

Microviscosity, defined as viscosity of the inner core of self-aggregates, can be determined by measuring the molecular anisotropy (*r*) resulting from the restricted rotational motion of DPH. The higher *r* value with increasing molecular weight of chitosan indicates the enhanced rigidity of hydrophobic domain of DAMC self-aggregates (Table 1). The mean diameter of DAMC self-aggregate was mainly dependent on the molecular weight of chitosan and was in the range of 130−300 nm with unimodal size distribution (Table 1).

Structure of DAMC Self-Aggregates. Figure 3 represents the anisotropy value (*r*) of DPH measured at different concentrations of DAMC self-aggregates with different molecular weights. The *r* values abruptly increased near *cac*, probably due to the dye-induced self-aggregate formation, and the values remained almost constant above *cac* independent of the self-aggregate concentration, except for DAMC200k. One interesting finding in this experiment is the increased *r* value of DAMC200k with increasing micelle concentrations. This might indicate a transition of self-aggregate shape from bamboolike cylindrical structure to a poorly organized birdnestlike structure. This could possibly be the case because the DAMC molecules have chain rigidity to a great extent, arising from the rigidity of parent chitosan and bulky deoxycholic acid groups. On the basis of the assumption that a single chain forms a conventional structure of a self-aggregate (i.e., spherical unimer), the diameter of an expected self-aggregate (d_{cal}) can be calculated by considering the length of monomer unit of chitosan (ca. 4 Å) and the molecular weight of chitosan. Therefore, the ratio between the measured and calculated diameter of self-aggregates (d_{real}/d_{cal}) could suggest the minimum aggregation number necessary to assemble a self-aggregate of spherical shape. Table 1 shows the existence of the calculated aggregation number (d_{real}/d_{cal}), which implies the formation of nonspherical self-aggregates above molecular weight of 40 kDa. Computer-simulated structure of chitosan and DAMC also supports the previous results. Indeed, Figure 4 shows that it is very difficult for the chitosan molecule itself to coil due to its chain rigidity (Figure 4a). When chitosan is modified with deoxycholic acid, DAMC chains tend to kink due to some intramolecular interaction at low concentration (Figure 4b). However, when DAMC concentrations increase, DAMC chains tend to be straightened due to the intermolecular interactions with concurrent self-association of deoxycholic acid units of neighboring DAMC chains (Figures 4c and 4d). By this way, the DAMC self-aggregates may form a cylindrical bamboolike structure, particularly when the molecular weight of chitosan backbone in DAMC is higher than 40 kDa. Even when the molecular weight is lower than 40 kDa, the micellar structure of DAMC may not be in the form of perfect sphere that has been commonly reported for the self-aggregates of poly(ethylene oxide) (PEO) based diblock copolymer that has high chain flexibility. This might be attributed to the rigidity of chitosan chains, likely due to the 1,4-β-glycosidic linkages and/or possible existence of multicore structure (rather than one) as previously reported (*10*), resulting in the formation of pseudosphere that might be formed very similar to the way of construction of a birdnest with debris of a tree.

Complex Formation between DAMC Self-Aggregates and DNA. One interesting feature of chitosan is its cationic character due to the amino group in each repeating unit. Therefore, DAMC self-aggregates were expected to form complexes with DNA, a representative anionic macromolecule existing in nature. The electrophoretic mobility of DNA, complexed with DAMC self-aggregates, decreased gradually on the agarose gel with increasing the molecular weight of DAMC at the same charge ratio (Figure 5). The addition of low molecular weight of DAMC5k self-aggregates, however, could not result in complete retardation of DNA even at higher charge ratios (data not shown). This could be attributed to the lower stability of DAMC5k self-aggregates (Figure 3). A similar behavior of complex formation was also confirmed by a fluorometer using ethidium bromide (EtBr) as a probe (Figure 6). The fluorescence intensity of EtBr was normalized by the intensity in the presence of DNA only. This loss in the fluorescence intensity indicates the condensation of DNA and the compaction of the complex particle, which could result in the exclusion of EtBr from DNA. The decrease in the fluorescence intensity was dependent on the molecular weight of DAMC. DAMC5k self-aggregates did not show the dramatic reduction in the fluorescence intensity after complexation with DNA, irrespective of charge ratios. However, the complexes from higher molecular weight DAMC were stable, and no significant change in the fluorescence intensity was observed over the charge ratio of 4.

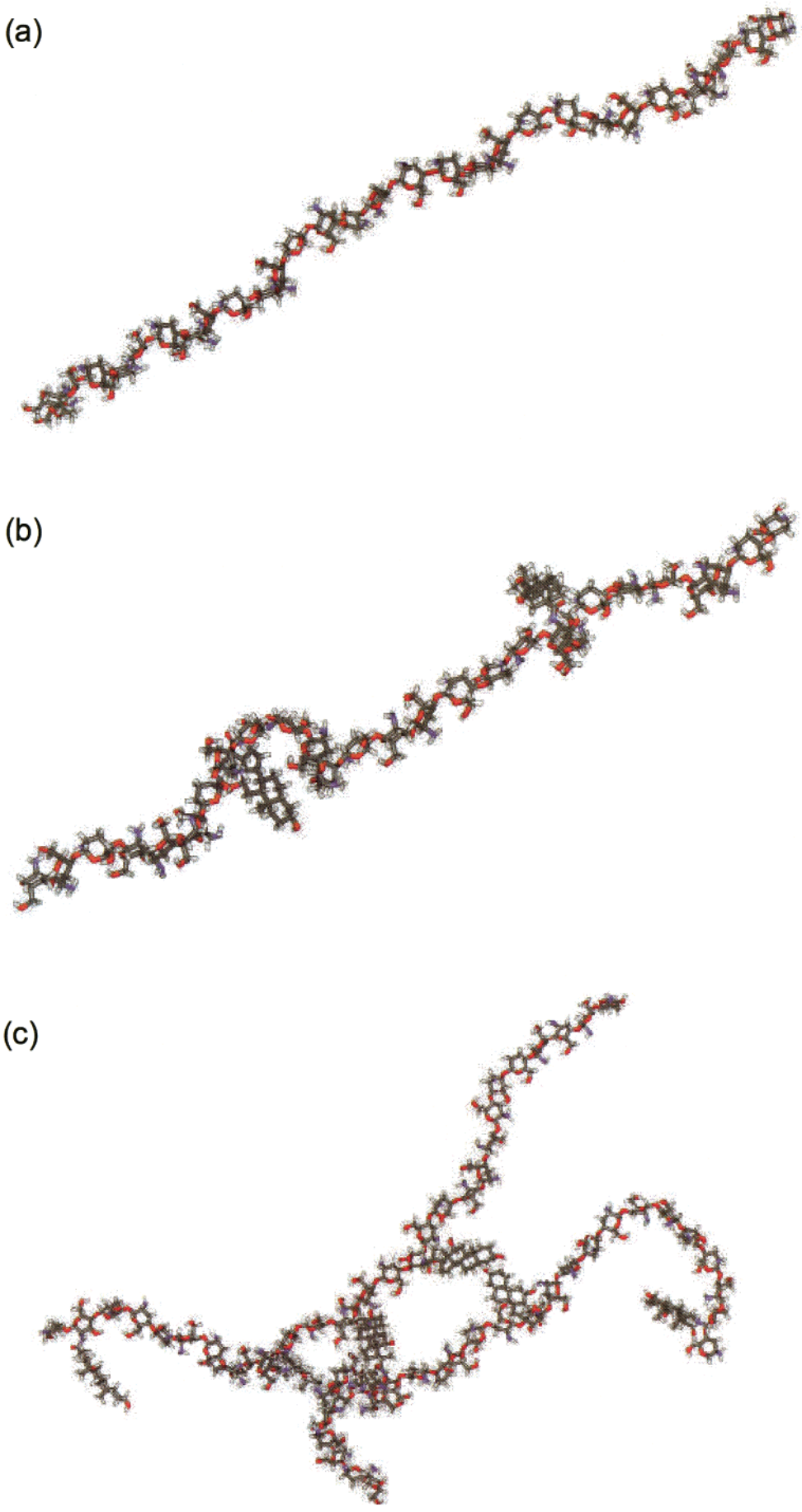
(a)
(b)
(c)

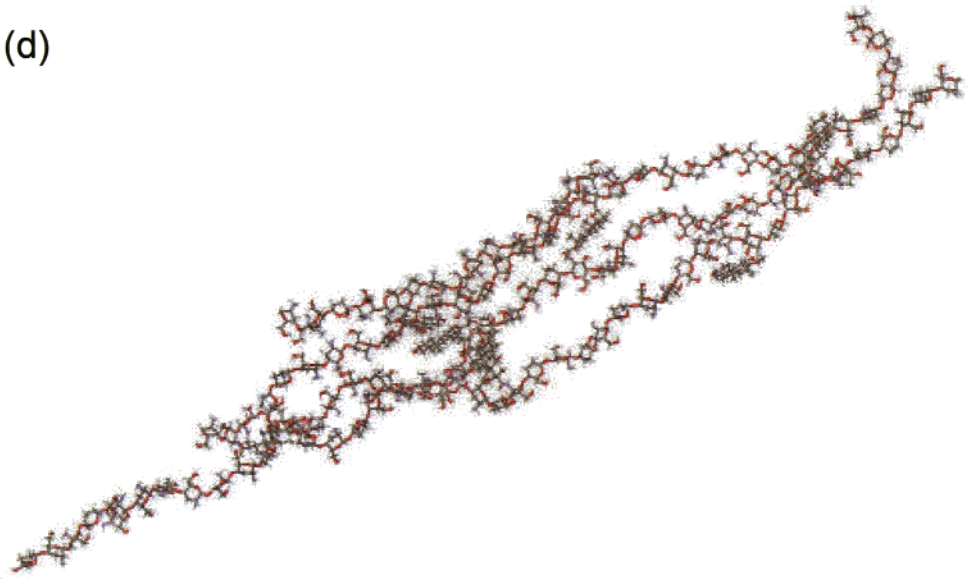

Figure 4. Simulated structure of (a) chitosan, (b) DAMC, (c) and (d) assembled self-aggregates formed by two and four DAMC molecules, respectively.

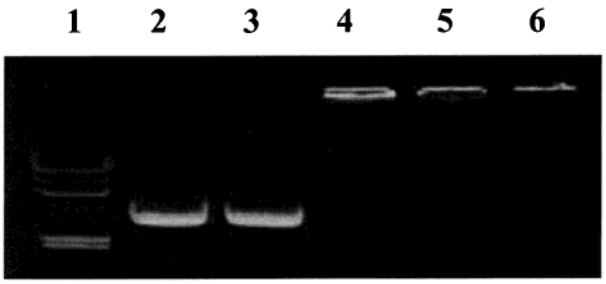

Figure 5. Electrophoresis of DAMC self-aggregate/DNA complexes on an agarose gel. Lane 1, DNA molecular weight marker; lane 2, DNA only; lane 3, DAMC5k/DNA complex; lane 4, DAMC25k/DNA complex; lane 5, DAMC40k/DNA complex; lane 6, DAMC200k/DNA complex at the charge ratio (±) of 4/1.

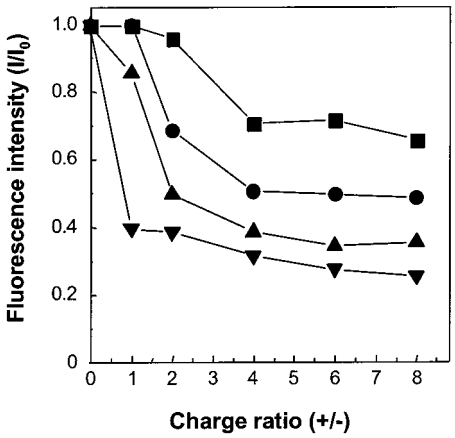

Figure 6. Changes in the fluorescence intensity of ethidium bromide in the presence of DAMC self-aggregate/DNA complexes as a function of charge ratios (■, DAMC5k; ●, DAMC25k; ▲, DAMC40k, ▼, DAMC200k).

In Vitro Transfection Efficiency. The transfection of COS-1 cells with DAMC self-aggregate/DNA complexes were studied next. The complexes at a charge ratio of 4 were chosen, as it was considered stable (Figures 5 and 6). In the absence of serum, it is evident that DAMC40k was the most efficient to deliver DNA to COS-1 cells, whereas DAMC5k self-aggregates showed the lowest

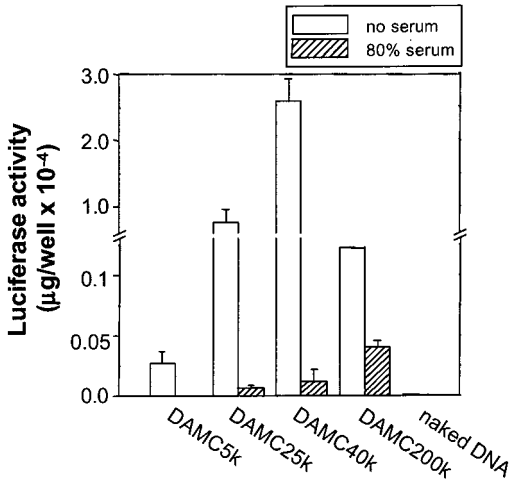

Figure 7. In vitro transfection activity of DAMC self-aggregate/pCMV−Luc+ complexes in COS-1 cells. Gene expression was determined by luciferase activity using a Promega kit.

transfection efficiency, likely due to the low stability of the complexes (Figure 7). Although DAMC5k self-aggregate slightly condenses the plasmid DNA from the measurement of the fluorescence intensity of EtBr (Figure 6), the DAMC5k self-aggregate/DNA complex does not seem to be strong enough at physiological ionic strength. DAMC200k self-aggregates could form highly condensed complexes with DNA. However, the complexes might have been too tight to release DNA. In the presence of serum, the transfection efficiency increased with increasing the molecular weight of DAMC due to the abundant proteins, which may act as an inhibitor of complex formation, resulting in weakening the ionic interaction between DAMC self-aggregates and DNA. Therefore, the optimum condition for cell transfection could be controlled using DAMC self-aggregates with different physicochemical properties including the size and structures.

CONCLUSIONS

Consideration of information generated in this analysis lead us to believe that structure of deoxycholic acid-

modified chitosan self-aggregate is dependent on the molecular weight of chitosan, and the condition of gene transfection is correlated to the structure of self-aggregates. This approach to control the size and structure of self-aggregates may find wide utility in the development of gene carriers, as well as many drug delivery applications.

ACKNOWLEDGMENT

Y.H.K. and C.R.P. are grateful for the financial support from Korea Science and Engineering Foundation (KOSEF) through Hyperstructured Organic Materials Research Center (HOMRC) of Seoul National University.

LITERATURE CITED

(1) Stolnik, S., Illum, L., and Davis, S. S. (1995) Long Circulating Microparticulate Drug Carriers. *Adv. Drug Deliv. Rev. 16*, 195−214.

(2) Kreuter, J. (1994) Nanoparticles. *Colloidal Drug Delivery Systems* (J. Kreuter, Ed.) pp 219−342, Marcel Dekker: New York.

(3) Yasugi, K., Nakamura, T., Nagasaki, Y., Kato, M., and Kataoka, K. (1999) Sugar-installed Polymer Micelles: Synthesis and Micellization of Poly(ethylene glycol)-Poly(D,L-lactide) Block Copolymers Having Sugar Groups at the PEG Chain End. *Macromolecules 32*, 8024−8032.

(4) Yokoyama, M. (1992) Block Copolymers as Drug Carriers. *Crit. Rev. Ther. Drug Carrier Sys. 9*, 213−248.

(5) Allen, C., Maysinger, D., and Eisenberg, A. (1999) Nano-engineering Block Copolymer Aggregates for Drug Delivery. *Colloid Surfaces B-Biointerfaces 16*, 3−27.

(6) Harada, A., and Kataoka, K. (1999) Chain Length Recognition: Core−Shell Supramolecular Assembly from Oppositely Charged Block Copolymers. *Science 283*, 65−67.

(7) Inoue, T., Chen, G. H., Nakamae, K., and Hoffman, A. S. (1998) An AB Block Copolymer of Oligo(methyl methacrylate) and Poly(acrylic acid) for Micellar Delivery of Hydrophobic Drugs. *J. Controlled Release 51*, 221−229.

(8) Yang, Y. W., Yang, Z., Zhou, Z. K., Attwood, D., and Booth, C. (1996) Association of Triblock Copolymers of Ethylene Oxide and Butylene Oxide in Aqueous Solution. A Study of B(n)E(m)B(n) Copolymers. *Macromolecules 29*, 670−680.

(9) Nishikawa, T., Akiyoshi, K., and Sunamoto, J. (1994) Supramolecular Assembly Between Nanoparticles of Hydrophobized Polysaccharide and Soluble-Protein Complexation between the Self-Aggregate of Cholesterol-Bearing Pullulan and α-Chymotrypsin. *Macromolecules 27*, 7654−7659.

(10) Lee, K. Y., Jo, W. H., Kwon, I. C., Kim, Y.-H., and Jeong, S. Y. (1998) Structural Determination and Interior Polarity of Self-Aggregates Prepared from Deoxycholic Acid-Modified Chitosan in Water. *Macromolecules 31*, 378−383.

(11) Qiu, Y. X., Zhang, T. H., Ruegsegger, M., and Marchant, R. E. (1998) Novel Nonionic Oligosaccharide Surfactant Polymers Derived from Poly(vinylamine) with Pendant Dextran and Hexanoyl Groups. *Macromolecules 31*, 165−171.

(12) Mulligan, R. C. (1993) The Basic Science of Gene-Therapy. *Science 260*, 926−932.

(13) Anderson, W. F. (1998) Human Gene Therapy. *Nature 392*(suppl.), 25−30.

(14) Haensler, J., and Szoka, F. C. (1993). Polyamidoamine Cascade Polymers Mediate Efficient Transfection of Cells in Culture. *Bioconjugate Chem. 4*, 372−379.

(15) Felgner, J. H., Kumar, R., Sridhar, C. N., Wheeler, C. J., Tsai, Y. J., Border, R., Ramsey, P., Martin, M., and Felgner, P. L. (1994) Enhanced Gene Delivery and Mechanism Studies with a Novel Series of Cationic Lipid Formulations. *J. Biol. Chem. 269*, 2550−2561.

(16) Kim, J.-S., Maruyama, A., Akaike, T., and Kim, S. W. (1997) In Vitro Gene Expression on Smooth Muscle Cells Using a Terplex Delivery System. *J. Controlled Release 47*, 51−59.

(17) Midoux, P., and Monsigny, M. (1999) Efficient Gene Transfer by Histidylated Polylysine pDNA Complexes. *Bioconjugate Chem. 10*, 406−411.

(18) Fischer, D., Bieber, T., Li, Y. X., Elsasser, H. P., and Kissel, T. (1999) A Novel Non-Viral Vector for DNA Delivery Based on Low Molecular Weight, Branched Polyethylenimine: Effect of Molecular Weight on Transfection Efficiency and Cytotoxicity. *Pharm. Res. 16*, 1273−1279.

(19) Hirano, S., Seino, H., Akiyama, H., and Nonaka, I. (1990) Chitosan: A Biocompatible Materials for Oral and Intravenous Administration. *Progress in Biomedical Polymers* (C. G. Gebelein, R. L. Dunn, Eds.) pp 283−290, Plenum Press, New York.

(20) Lee, M., Nah, J. W., Kwon, Y., Koh, J. J., Ko, K. S., and Kim, S. W. (2001) Water-Soluble and Low Molecular Weight Chitosan-based Plasmid DNA Delivery. *Pharm. Res. 18*, 427−431.

(21) Richardson, S. C. W., Kolbe, H. J. V., and Duncan, R. (1999) Potential of Low Molecular Mass Chitosan as a DNA Delivery System: Biocompatibility, Body Distribution and Ability to Complex and Protect DNA. *Int. J. Pharm. 178*, 231−243.

(22) Roy, K., Mao, H. Q., Huang, S. K., and Leong, K. W. (1999) Oral Gene Delivery with Chitosan-DNA Nanoparticles Generates Immunologic Protection in a Murine Model of Peanut Allergy. *Nature Medicine 5*, 387−391.

(23) MacLaughlin, F. C., Mumper, R. J., Wang, J. J., Tagliaferri, J. M., Gill, I., Hinchcliffe, M., and Rolland, A. P. (1998) Chitosan and Depolymerized Chitosan Oligomers as Condensing Carriers for In Vivo Plasmid Delivery. *J. Controlled Release 56*, 259−272.

(24) Lee, K. Y., Kwon, I. C., Kim, Y.-H., Jo, W. H., and Jeong, S. Y. (1998) Preparation of Chitosan Self-Aggregates as a Gene Delivery Carrier. *J. Controlled Release 51*, 213−220.

(25) Sannan, T., Kurita, K., and Iwakura, Y. (1976) Studies on Chitin. 2. Effect of Deacetylation on Solubility. *Makromol. Chem. 177*, 3589−3600.

(26) Wilhelm, M., Zhao, C. L., Wang, Y. C., Xu, R. L., Winnik, M. A., Mura, J. L., Riess, G., and Croucher, M. D. (1991) Polymer Micelle Formation. 3. Poly(styrene-ethylene oxide) Block Copolymer Micelle Formation in Water − A Fluorescence Probe Study. *Macromolecules 24*, 1033−1040.

(27) Nair, P. P., and Kritchevsky, D. (1971) *The Bile Acids, Chemistry, Physiology, and Metabolism*, Plenum Press: New York.

(28) Ringsdorf, H., Venzmer, J., and Winnik, F. M. (1991) Fluorescence Studies of Hydrophobically Modified Poly(*N*-Isopropylacrylamides). *Macromolecules 24*, 1678−1686.

(29) Kim, T. W., Chung, H., Kwon, I. C., Sung, H. C., and Jeong, S. Y. (2001) Optimization of Lipid Composition in Cationic Emulsion as In Vitro and In Vivo Transfection Agents. *Pharm Res. 18*, 54−60.

(30) Hermanson, G. T., Mallia, A. K., and Smith, P. K. (1992) *Immobilized Affinity Ligand Techniques*, Academic Press, San Diego.

BC015510C